Synthesis and Electrical Properties of Polyaniline/Polyaniline Grafted Multiwalled Carbon Nanotube Mixture via *In Situ* Static Interfacial Polymerization

IN-YUP JEON,[1] LOON-SENG TAN,[2] JONG-BEOM BAEK[1]

[1]School of Energy Engineering, Ulsan National Institute of Science and Technology (UNIST), 194, Banyeon, Ulsan 689-801, South Korea

[2]Nanostructured and Biological Materials Branch, Materials and Manufacturing Directorate, U.S. Air Force Research Laboratory, AFRL/RXBN, Wright-Patterson AFB, Ohio 45433

Received 5 December 2009; accepted 24 January 2010
DOI: 10.1002/pola.23963
Published online in Wiley InterScience (www.interscience.wiley.com).

ABSTRACT: The mixture of polyaniline (PANi) and PANi grafted multiwalled carbon nanotube (PANi-*g*-MWNT) was prepared by a two-step reaction sequence. MWNT was first functionalized with 4-aminobenzoic acid via "direct" Firedel-Crafts acylation in polyphosphoric acid (PPA)/phosphorous pentoxide (P_2O_5) medium to afford 4-aminobenzoyl-functionalized MWNT (AF-MWNT). Then, aniline was polymerized via an *in situ* static interfacial polymerization in H_2O/CH_2Cl_2 in the presence of AF-MWNT in organic phase to yield the mixture of PANi and PANi-*g*-MWNT. The mixture was characterized with a various analytical techniques such as elemental analysis (EA), Fourier transform infrared spectroscopy (FTIR), wide angle X-ray diffraction (WAXD), scanning electron microscopy (SEM), transmission electron microscopy (TEM), thermogravimetric analysis (TGA), cyclic voltammogram (CV), UV-vis and fluorescence spectroscopies, and electrical conductivity measurement. On the basis of TGA analysis, the thermo-oxidative stability of the mixture was markably improved compared to that of PANi homopolymer. Even after dedoping, in alkaline solution, the mixture would still display semimetallic conductivity (4.9 S/cm). The capacitance of the mixture was also greatly enhanced and its capacitance decay with respect to cycle times was significantly reduced. © 2010 Wiley Periodicals, Inc. J Polym Sci Part A: Polym Chem 48: 1962–1972, 2010

KEYWORDS: conducting polymers; interfaces; nanocomposites

INTRODUCTION Conducting polymers have opened up many new possibilities for fabricating devices such as batteries, sensors, light-emitting diodes, and electrochromic displays.[1] Among them, polyaniline (PANi) is one of the most promising conducting polymers, because it can be easily prepared and possesses some unique properties. For example, its conductivity can be simply controlled by its doping level, which can be reversibly manipulated by an acid doping-base dedoping process.[2] In addition, PANi has relatively good processability and remarkable environmental stability.[3] Thus, PANi has been extensively studied as potential materials for anticorrosion coatings,[4] batteries,[5] sensors,[6] and antistatic coatings.[7]

Recently, nanostructured one-dimensional (1D) forms of PANi such as nanowires, nanorods, nanotubes, and nanofibers have attracted a lot of research interest owing to its metal-like conductivity, stemming from PANi's highly oriented molecular structure. As a result, 1D PANi has become an emerging material for nanoscale device applications.[8] Nanostructured 1D PANI can be synthesized chemically or electrochemically by template polymerization,[9] self-assembly,[10] emulsions polymerization,[11] dilute-solution polymerization[12] and interfacial polymerization.[13] Amongst them, interfacial polymerization is a straightforward route to controlling the morphology of nanofibers. Advantages of interfacial polymerization are:[1] it does not rely upon any specific template to control morphology;[2] high-quaility nanofibers can be obtained using mineral acid without salt contamination;[3] the formation of secondary structure can be effectively suppressed by the rapid diffusion of the ionic nanofibers from the interface of binary reaction medium into aqueous phase.[13,14]

The conductivity of PANi is generally originated from low-molar-mass mineral acid doping, while the reduced or neutral state of PANi is insulating material. However, the conductivity of doped PANi is decreased with passing time because mineral acid dopants tend to migrate to the surface and evaporate. As a result, the thicker polymer film is necessary to delay conductivity loss. In this case, charge transport would be slower in a multilayer device architecture.[15] This problem can be resolved by adding CNT into PANi as a dopant as well as conducting bridge. PANi is conjugated,

Additional Supporting Information may be found in the online version of this article. Correspondence to: J.-B. Baek (E-mail: jbbaek@unist.ac.kr)
Journal of Polymer Science: Part A: Polymer Chemistry, Vol. 48, 1962–1972 (2010)

Report Documentation Page

Form Approved
OMB No. 0704-0188

1. REPORT DATE	2. REPORT TYPE	3. DATES COVERED
2010		**00-00-2010 to 00-00-2010**

4. TITLE AND SUBTITLE
Synthesis and Electrical Properties of Polyaniline/Polyaniline Grafted Multiwalled Carbon Nanotube Mixture via In Situ Static Interfacial Polymerization

5a. CONTRACT NUMBER
5b. GRANT NUMBER
5c. PROGRAM ELEMENT NUMBER

6. AUTHOR(S)

5d. PROJECT NUMBER
5e. TASK NUMBER
5f. WORK UNIT NUMBER

7. PERFORMING ORGANIZATION NAME(S) AND ADDRESS(ES)
Ulsan National Institute of Science and Technology (UNIST),Interdisciplinary School of Green Energy & Inst of Advanced Materials & Devices,100, Banyeon,Ulsan 689-798, South Korea,

8. PERFORMING ORGANIZATION REPORT NUMBER

9. SPONSORING/MONITORING AGENCY NAME(S) AND ADDRESS(ES)

10. SPONSOR/MONITOR'S ACRONYM(S)
11. SPONSOR/MONITOR'S REPORT NUMBER(S)

12. DISTRIBUTION/AVAILABILITY STATEMENT
Approved for public release; distribution unlimited

13. SUPPLEMENTARY NOTES

14. ABSTRACT

The mixture of polyaniline (PANi) and PANi grafted multiwalled carbon nanotube (PANi-g-MWNT) was prepared by a two-step reaction sequence. MWNT was first functionalized with 4-aminobenzoic acid via ??direct?? Firedel-Crafts acylation in polyphosphoric acid (PPA)/phosphorous pentoxide (P2O5) medium to afford 4-aminobenzoyl-functionalized MWNT (AFMWNT). Then, aniline was polymerized via an in situ static interfacial polymerization in H2O/CH2Cl2 in the presence of AFMWNT in organic phase to yield the mixture of PANi and PANi-g-MWNT. The mixture was characterized with a various analytical techniques such as elemental analysis (EA), Fourier transform infrared spectroscopy (FTIR), wide angle X-ray diffraction (WAXD), scanning electron microscopy (SEM), transmission electron microscopy (TEM), thermogravimetric analysis (TGA), cyclic voltammogram (CV), UV-vis and fluorescence spectroscopies, and electrical conductivity measurement. On the basis of TGA analysis, the thermo-oxidative stability of the mixture was markably improved compared to that of PANi homopolymer. Even after dedoping, in alkaline solution, the mixture would still display semimetallic conductivity (4.9 S/ cm). The capacitance of the mixture was also greatly enhanced and its capacitance decay with respect to cycle times was significantly reduced.

15. SUBJECT TERMS

16. SECURITY CLASSIFICATION OF:			17. LIMITATION OF ABSTRACT	18. NUMBER OF PAGES	19a. NAME OF RESPONSIBLE PERSON
a. REPORT	b. ABSTRACT	c. THIS PAGE			
unclassified	**unclassified**	**unclassified**	**Same as Report (SAR)**	**11**	

electron-rich polymer, while CNT is conjugated electron-deficient material with outstanding properties such as aspect ratio, electrical conductivity, chemical stability, and good mechanical properties.[16] Indeed, previous works report that PANi/CNT composites prepared from physical blending have exhibited significant improvement in both mechanical and electrical properties.[17] However, the approaches that involve PANi wrapping around the surface of CNT via secondary interactions such as van der Waals attraction and hydrogen bonding used oxidized CNT. Such relatively interactions may not be the best option for the ultimate transfer of CNT properties to PANi. We believe that covalent links between CNT and PANi could serve better for maximum enhanced properties.

In this regard, we have functionalized multiwalled carbon nanotube (MWNT) with 4-amino benzoic acid via "direct" Friedel-Crafts acylation in a mild polyphosphoric acid (PPA)/phosphorous pentoxide (P_2O_5) medium. The resultant 4-aminobenzoyl-functionalized MWNT (AF-MWNT) is expected not only to provide reactive sites for PANi grafting, but also to improve CNT's chemical affinity with PANi for better dispersibility and compatibility. Although various methods for the functionalization of CNTs have been reported in literature, most cases required that CNTs were treated in corrosive and oxidizing mineral acids with or without sonication.[18] However, we strongly believe that most of foregoing approaches would have damaged CNT, resulting in oxidized CNT. It has been well known for more than 150 years that strong acids (specifically nitric acid) can oxidize graphite into graphite oxide,[19] which does not have electrical conductivity nor mechanical integrity. Since graphite, which has less bond strains and is chemically more stable than CNT, can be readily oxidized in strong acids, it follows that CNT should be even more easily oxidized, and indeed it is the case.[20] As a result, most of early research works produced CNT-based composites that were far from theoretically expected performance.

The reaction condition in this approach is known to be less destructive chemical modification.[21] Specifically, the polymeric mild acidic medium, PPA, would play two pivotal roles for both handling safety and reaction efficiency. They are:[1] PPA is mild enough not to damage, but still acidic enough to protonate CNT for deaggregation;[2] The high viscosity of polymeric PPA impedes reaggregation after the separation and isolation of individual CNT tubes and small CNT bundles (a few tubes together). Hence, damages must be diminished to preserve outstanding properties such as electrical, thermal and physical properties.[22]

The mixture of PANi and PANi grafted multiwalled carbon nanotubes (PANi-*g*-MWNT) (PANi/PANi-*g*-MWNT) was prepared without physical agitation via *in situ* static interfacial polymerization in H_2O/CH_2Cl_2 with AF-MWNT in organic phase and aniline and ammonium persulfate (APS) in acidic aqueous phase. The resultant PANi/PANi-*g*-MWNT mixture was expected to exhibit significant improvement on thermal and electrical properties over the reference PANi homopolymer. The approach is unique to demonstrate safe but the efficient chemical modification of MWNT and thus, the performance of resultant PANi/PANi-*g*-MWNT mixture is expected to be significantly enhanced.

EXPERIMENTAL

Materials

All reagents and solvents were purchased from Aldrich Chemical and Lancaster Synthesis, and used as received, unless otherwise specified. Multiwalled carbon nanotube (MWNT, CVD MWNT 95 with diameter of ~20 nm and length of 10–50 μm) was obtained from Hanwha Nanotech, Incheon, Korea.[23]

Instrumentation

Infrared (IR) spectra were recorded on Jasco FTIR 480 Plus spectrophotometer. Solid samples were imbedded in KBr disks. Elemental analyses (EA) were performed with a CE Instruments EA1110. Thermogravimetric analysis (TGA) was conducted in nitrogen and air atmospheres with a heating rate of 10 °C/min using a Perkin–Elmer TGA 7. The field emission scanning electron microscopy (FE-SEM) used in this work was LEO 1530FE. Samples were not sputtered with any metallic coating since as-received and functionalized MWNT are already good conductor. The field emission transmission electron microscope (FE-TEM) employed in this work was a FEI Tecnai G2 F30 S-Twin. The surface area was measured by nitrogen adsorption–desorption isotherms using the Brunauer-Emmett-Teller (BET) method using Micromeritics ASAP 2504N. Wide-angle X-ray diffraction (WAXD) powder patterns were recorded with a Rigaku RU-200 diffractometer using Ni-filtered Cu Kα radiation (40 kV, 100 mA, $\lambda = 0.15418$ nm). UV-vis spectra were obtained on a Perkin–Elmer Lambda 35 UV-vis spectrometer. Stock solutions were prepared by dissolving 10 mg of each sample in l L of *N*-methyl-2-pyrrolidone (NMP). Photoluminescence measurements were performed with a Perkin–Elmer LS 55 Fluorescence spectrometer. Cyclic voltammetry (CV) experiments were performed with a SI 1287 Electrochemical Interface (Solartron Analytical, UK). The test electrodes were prepared by dipping glassy carbon sheet into sample solution in *m*-cresol and the electrode was dried and used as working electrode. The CV experiment was conducted in 0.1 M aqueous sulfuric acid solution with a scan rate of 10 mV/s and in the potential of -0.25 and 1.25 V. The three-electrode system consisted of a glassy carbon electrode as working electrode, an Ag/AgCl (sat. KCl) as reference electrode and platinum gauze as counter electrode. All potential values are reported as a function of Ag/AgCl. The resistance of samples was measured by four point probe method using Advanced Instrument Technology (AIT) CMT-SR1000N with Jandel Engineering probe at room temperature. All test specimens were prepared by compression mold with high pressure at 60 MPa, and the conductivity values were the averages of 10 measurements.

Functionalization of MWNT (AF-MWNT)

Into a resin flask equipped with high torque mechanical stirrer, nitrogen inlet and outlet, 4-aminobenzoic acid (10.0 g, 73 mmol), MWNT (5.0 g), PPA (300.0 g, 83% P_2O_5 assay) and P_2O_5 (75.0 g) were placed. The flask immersed in an oil bath and the reaction mixture was stirred and gently heated at 100 °C for 1 h. Then the reaction mixture was heated and

maintained around 130 °C for 72 h under nitrogen atmosphere. The dark homogeneous mixture was precipitated into water. The precipitates were collected by suction filtration and Soxhlet extracted with distilled water for three days and methanol for three days, and finally freeze-dried for 48 h to afford 9.82 g (71.7% yield) dark black powder.

Interfacial Polymerization of PANi

Aniline (40.0 g, 0.430 mol) was dissolved in CH_2Cl_2 (100 mL). APS (24.5 g, 0.107 mol) was dissolved in 500 mL of 1.0 M HCl aqueous solution. In a 1.0 L beaker, aniline/CH_2Cl_2 solution was charged and then APS/1.0 M HCl solution was very slowly added. The two-phase solution was placed at room temperature without agitation for 24 h. The color of aniline/CH_2Cl_2 solution (bottom layer) was changed from colorless to light brown. The color of APS/1.0 M HCl solution (top layer) was changed from pinkish to dark green. At the end of polymerization, the resulting dark green solid was collected by filtration. The product was repeatedly washed with distilled water and methanol. The resultant solids were transferred to an extraction thimble and Soxhlet extracted with distilled water for three days and methanol for three days, and finally freeze-dried under reduced pressure for 48 h to give 9.9 g (25% yield) of dark green powder.

Synthesis of PANi/PANi-*g*-MWNT Mixture

Into the solution containing aniline (18.0 g, 0.193 mol) in CH_2Cl_2 (50 mL), AF-MWNT (2.0 g) was dispersed. APS (12.5 g, 0.055 mol) was dissolved in 250 mL of 1.0 M HCl aqueous solution. In a 1.0 L beaker, aniline/AF-MWNT/CH_2Cl_2 solution was charged and then APS/1.0 M HCl solution was very slowly added. The rest of reaction and work-up procedures were similar to PANi. The color of aniline/AF-MWNT/CH_2Cl_2 solution was from dark black to light brown. The resulting dark green precipitates in top aqueous layer were collected by filtration. The product was repeatedly washed with distilled water and methanol. The resultant solids were transferred to an extraction thimble and Soxhlet extracted with distilled water for three days and methanol for 3 days, and finally freeze-dried under reduced pressure for 48 h to give 5.80 g (32% yield) of dark green powder.

Dedoping PANi and PANi/PANi-*g*-MWNT

The PANi and PANi/PANi-*g*-MWNT were converted into the base form by immersion in excess of 1 M aqueous ammonium hydroxide at room temperature for 24 h. The samples were collected by filtration, washed with distilled water, and finally freeze-dried for 48 h.

RESULTS AND DISCUSSION

Aminobenzoyl-Functionalized MWNT

As described in our previous reports,[21(a,c),24] the functionalization of MWNT was carried out with 4-aminobenzoic acid in PPA/P_2O_5 medium at 130 °C to afford aminobenzoyl-functionalized MWNT (AF-MWNT) [Fig. 1(a)]. To minimize unexpected variables, the resultant AF-MWNT was completely worked up in the Soxhlet extraction in water for 3 days to remove any residual reaction medium and methanol for three days to get rid of low molar mass impurities. The functionalization of MWNT was conveniently monitored by FTIR [Fig. 1(b)]. Pristine MWNT displayed featureless FTIR spectrum at nomal magnification. However, in the zoomed-in region of the spectra, there are sp^2C—H and sp^3C—H stretching bands at 2924 cm^{-1} [Fig. 1(b), inset]. The peak is attributed by the defects at sidewalls and open ends of MWNTs.[25] These defects should be originated from the synthetic process of MWNT with hydrocarbon feedstock.[26] AF-MWNT clearly showed an aromatic carbonyl (C=O) peak at 1644 cm^{-1}, whose value was shifted from 1666 cm^{-1} of carboxylic acid in 4-aminobenzoic acid. The functionalization of MWNT was further confirmed by SEM imaging. Pristine MWNT shows that the tubes have seamless and smooth surfaces with the average diameter of 10–20 nm [Fig. 1(c)]. Thus, the average diameter of AF-MWNT is increased to ~40–50 nm [Fig. 1(d)]. Considering the length of 4-aminobenzoyl moiety, which is ~1 nm, the average diameter of AF-MWNT should be in the range of 12–22 nm. The unexpected larger diameter is likely due to the bundling of polar AF-MWNT. Similar bundling phenomenon was observed in hydroxyl-functionalized MWNT (HF-MWNT).[21(c)] The driving force for bundling of polar surface groups of functionalized MWNT could stem from stronger epitaxial interaction than van der Waals attraction of pristine MWNT. Unlike single walled carbon nanotubes (SWNT) which characteristically form "ropes," MWNT has much less tendency to bundle because of its rigidity. However, when epitaxial interaction is strong enough to overcome the structural rigidity, MWNT is forced to bundle along the lateral surface. Specifically, AF- and HF-MWNT are able to form strong hydrogen bonding. Fortuitously, the average diameter dimension of bundled AF-MWNT in the SEM image is ~40–50 nm, which agreed well with the diameter of a bundle containing four AF-MWNTs [Fig. 1(d)]. The result is similar with HF-MWNT.[21(c)] To confirm this scenario, AF-MWNT was dispersed in methanesulfonic acid (MSA) to individualize AF-MWNT and diluted in large amount of *N*-methyl-2-pyrrolidone (NMP). TEM grid was dipped into the dilute solution and vacuum dried, and with it were obtained TEM images, which clearly showed individual tubes with diameter dimension of 20 nm [Fig. 1(e,f)].

To determine the amount of 4-aminobenzoyl moiety, the powder samples were subjected to thermogravimetric analysis (TGA). The weight loss of AF-MWNT was ~48% around 660 °C, at which the two curves from pristine MWNT and AF-MWNT crossed [Fig. 1(g)]. The weight loss was attributed to thermally stripping off of 4-aminobenzoyl moiety on MWNT surface. It strongly implied that a large amount of 4-aminobenzoyl moieties was covalently attached to the surface of AF-MWNT. Interestingly, the thermo-oxidative stability of AF-MWNT above 660 °C is higher than pristine MWNT [pink oval area in Fig. 1(g)]. This is an evidence for the presence of surface aromatic hydrocarbon source to repair defects on MWNT surface during charring at high temperature.[27] Furthermore, the theoretical and experimental CHN contents of AF-MWNT were also in agreement (Table 1). Therefore, MWNT was successfully decorated by 4-aminobenzoyl moieties, which could be useful sites to covalently link various materials via addition reaction.

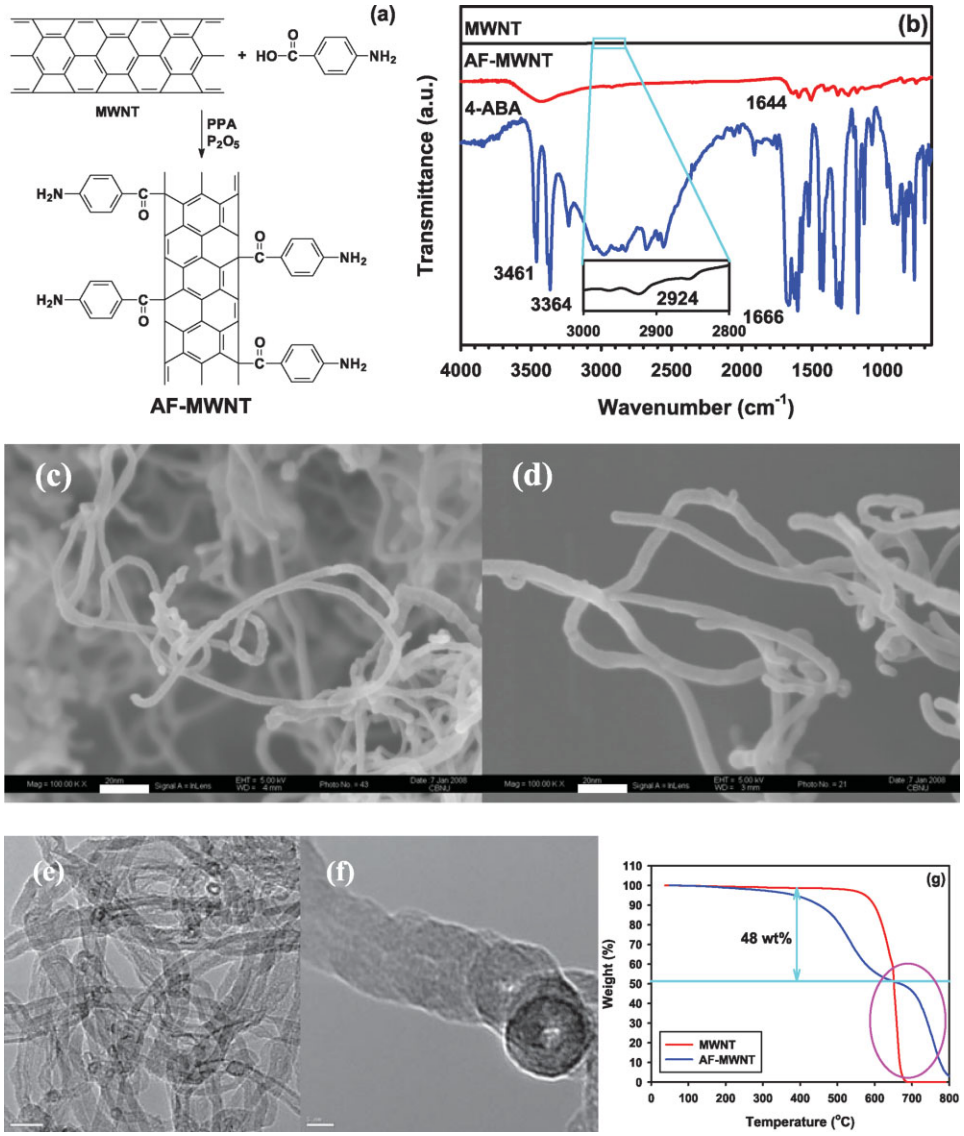

FIGURE 1 (a) Functionalization of MWNT with 4-aminobenzoic acid in polyphosphoric acid (PPA)/phosphorous pentoxide (P_2O_5) to afford 4-aminobenzoyl-functionalized MWNT (AF-MWNT); (b) FTIR (KBr pellet) spectra of as-received MWNT, AF-MWNT and 4-aminobenzoic acid; (c) SEM image of as-received MWNT (100,000×, scale bar is 100 nm); (d) SEM image of AF-MWNT (100,000×, scale bar is 100 nm); (e) TEM image of AF-MWNT at lower magnification (scale bar is 20 nm); (f) TEM image of AF-MWNT at higher magnification (scale bar is 5 nm); (g) TGA thermograms of MWNT and AF-MWNT in air with heating rate of 10 °C/min, showing that 48 wt % of 4-aminobenzoyl (AF-) moiety is grafted on the surface of MWNT. [Color figure can be viewed in the online issue, which is available at www.interscience. wiley.com.]

Grafting of PANi Onto AF-MWNT

Polyaniline (PANi) can be covalently decorated onto the surface of AF-MWNT via *in situ* static interfacial polymerization in H_2O/CH_2Cl_2.[23] The reaction condition was the same as oxidative synthesis of PANi except with CH_2Cl_2 as an additional (organic) solvent phase. APS and hydrochloric acid are in the top aqueous phase. The AF-MWNT and aniline stay in the bottom organic phase. The hydrochloric acid doped (protonated) PANi migrates to aqueous phase (see Supporting Information Fig. S1). Similarly, interfacial polymerization in the presence of AF-MWNT was carried out without physical agitation (static interfacial polymerization) [Fig. 2(a)]. As polymerization was occurring at the interface, protonated PANi homopolymer and PANi-*g*-MWNT would diffuse into the top aqueous phase. As a result, the product in aqueous phase should consist of PANi/PANi-*g*-MWNT mixture. The black residue at the bottom of organic phase [white arrow in Fig. 2(a)] was identified as the unreacted AF-MWNT. The amount of AF-MWNT incorporated into the reaction could be estimated from residual AF-MWNT on the bottom of vial [Fig. 2(b)], which was 45%. Hence, AF-MWNT incorporated into grafting reaction to afford PANi-*g*-MWNT was 55%. The value was reproducible for *in situ* static interfacial polymerization. However, when physical agitation was applied (dynamic interfacial polymerization), no residual AF-MWNT could be visually detected at the bottom of organic phase [see Supporting Information Fig. S2(a)]. Due to the fact that the doping level of hydrochloric acid in PANi is unknown, the CHN contents cannot be accurately calculated (Table 1). However, the carbon content of PANi was increased by more than 11% after Soxhlet extraction with water, indicating that the extraction could significantly remove hydrochloric acid from the sample. The carbon content was further increased after immersion into aqueous ammonium hydroxide (dedoping). Still, theoretical and empirical carbon contents were ~5% in descrepancy (Table 1). We believe that the

TABLE 1 Elemental Analysis of Samples

Sample	State	CF	FW (g/mol)		C (%)	H (%)	N (%)
MWNT	As-received	C	12.01	Calcd.	100	0.00	0.00
				Found	94.55	0.06	0.01
AF-MWNT	As-prepared[a]	$C_{12.71}H_6NO$	189.93	Calcd.	80.90	3.21	7.42
				Found	79.06	2.20	5.45
PANi	As-prepared	NA	NA	Found	60.04	4.66	10.35
	After Soxhlet Extraction	NA	NA	Found	71.47	4.76	13.03
	Dedoped	$C_6H_{-5}N$	91.11	Calcd.	79.10	5.53	15.37
				Found	74.15	4.74	13.10
PANi/PANi-*g*-MWNT	As-prepared	NA	NA	Found	70.95	3.10	6.91
	After Soxhlet Extraction	NA	NA	Found	78.62	2.80	6.94
	Dedoped[a]	$C_{90.29}H_{65.47}N_{12.89}O$	1347.1	Calcd.	80.50	4.91	13.40
				Found	76.31	3.14	8.40

CF, chemical formula; FW, formula weight; NA, not available.
[a] Calculate based on 55 wt % of AF-MWNT, which had been incorporated into the reaction.

entrapped hydrochloric acid could not be completely removed even after dedoping in aqueous ammonium hydroxide. In the case of PANi/PANi-*g*-MWNT mixture, carbon content was increased by 8% after Soxhlet extraction, but it was 2.3% decreased after dedoping. The nitrogen content was noticeably increased probably due to the entrapped ammonia. Nevertheless, overall CHN contents agreed well between theoretical and experimental values for PANi/PANi-*g*-MWNT (Table 1).

FTIR Study

The PANi homopolymers displayed the characteristic bands of secondary amine (N—H) at 3235 cm^{-1}, the C=C stretching deformation of the quinoid structure at 1571 cm^{-1}, benzenoid rings at 1500 cm^{-1} and the C—N stretching band of the secondary aromatic amine at 1291 cm^{-1} [Fig. 3(a)] The PANi/PANi-*g*-MWNT sample displayed almost identical characteristic bands at 3237, 1592, 1500, and 1303 cm^{-1}. Compared to the number of PANi repeating units in PANi-*g*-MWNT composite, the relative population of C=O groups, which were only located at the covalent junctions between AF-MWNT and PANi, was too low to be clearly discerned.

Wide-Angle X-Ray Diffraction (WAXD)

To determine the crystalline or amorphous nature of materials, wide-angle X-ray diffraction (WAXD) was used. Soxhlet-extracted powder samples were subjected to WAXD scans. The AF-MWNT displayed *d*-spacing values at 2.10 ($2\Theta = 43.10^\circ$), 2.95 ($2\Theta = 30.33^\circ$) and 3.44 Å ($2\Theta = 25.92^\circ$). The peak at 3.47 Å was also related to wall-to-wall distance of MWNTs [Fig. 3(a)]. The PANi showed a broad peak at $2\Theta \approx 20.0^\circ$ and 1 weak crystalline peak at 30.34° [Fig. 3(b)]. This very broad diffraction is typical pattern of an amorphous phase.[28] It was an indication that major portion of PANi homopolymer was consisted of an amorphous phase. It has also been reported that the crystallinity of PANi would increase after doping with HCl.[29] That means the dopont should affect the crystal structure and crystallinity of PANi. Accordingly, amorphous phase of PANi represented that most of bounded HCl had been removed during Soxhlet extraction for several days with distilled water and methanol (see Experimental section).

PANi/PANi-*g*-MWNT mixture showed much weaker amorphous peak at $2\Theta \approx 20.0^\circ$. The mixture displayed strong crystalline peaks at 26.06, 30.32, and 42.92° even after HCl dopant was mostly removed during Soxhlet extraction. The higher crystallinity of PANi/PANi-*g*-MWNT mixture than that of PANi was probably because covalently linked MWNT provided nucleation sites for PANi crystallization.

Scanning Electron Microscopy (SEM)

Interfacial polymerization is an effective method to suppress the secondary growth of PANi structure.[30] The resultant PANi homopolymer appears in the form of nanofibers with an average diameter of 20 nm and length of several tens of μm [Fig. 4(a,b)]. As expected, PANi was not completely grafted, and free PANi coexists with PANi-*g*-MWNT [Fig. 4(c,d)]. It can be discerned PANi-*g*-MWNT from PANi nanofibers [Fig. 4(c)]. The morphology of PANi nanofibers in the PANi/PANi-*g*-MWNT mixture is similar to that of PANi homopolymer [Fig. 4(c)]. The average diameter of PANi-*g*-MWNT is approximately 80–90 nm, which is profoundly larger than that of PANi nanofibers [20 nm, see Fig. 4(b)] as well as AF-MWNT bundles [40 nm, see Fig. 1(d)]. The result strongly suggested that some portion of PANi grafted onto the surface of AF-MWNT [Fig. 4(d), arrow 1 and 2]. When both PANi homopolymer and PANi/PANi-*g*-MWNT mixture were prepared from dynamic interfacial polymerization (with physical agitation) [see Supporting Information Fig. S2(a)], the morphologies are significantly different from those prepared by static interfacial polymerization [see Supporting Information Fig. S2(b,c)]. Specifically, PANi nanofibers show much less ordered structure [see Supporting Information Fig. S2(b)]. The structures of PANi prepared from both static and dynamic interfacial polymerizations are also far different from that of

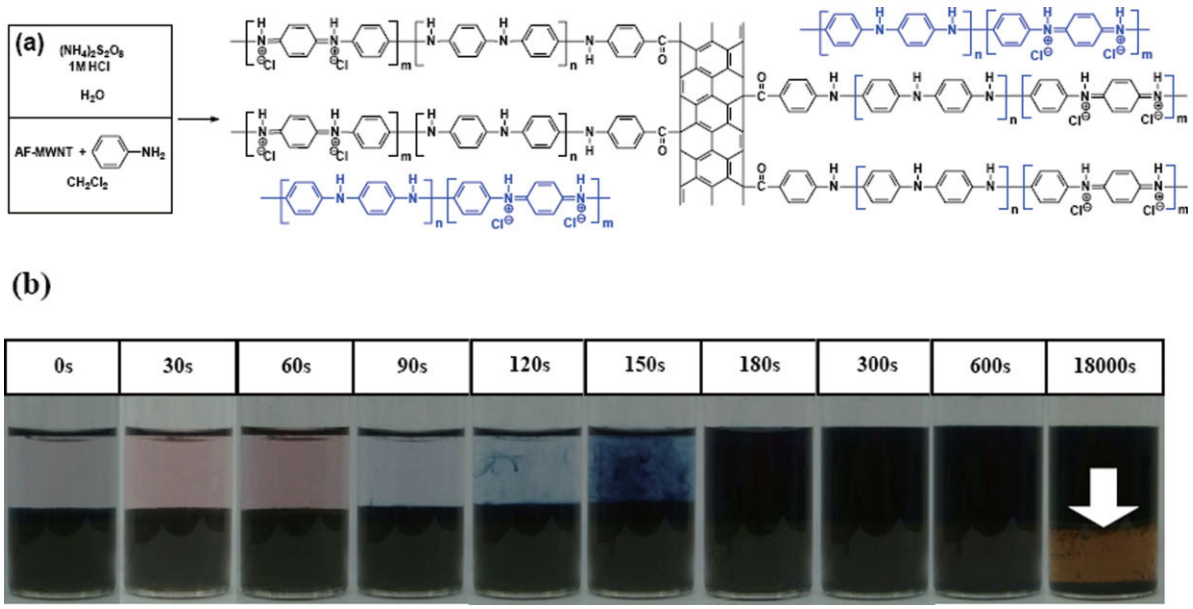

FIGURE 2 (a) Interfacial polymerization of aniline: top aqueous 1 M hydrochloric acid layer contains ammonium persulfate (APS); bottom organic layer contains aniline and AF-MWNT; (b) photographs of reaction vials as function of reaction time. As static interfacial polymerization was progressed, the color of top aqueous layer turned to darker and that of bottom organic layer containing AF-MWNT turned to lighter. The amount of AF-MWNT incorporated into the reaction could be estimated by residual amount of AF-MWNT on the bottom of vial (white arrow), which was 45%. Hence, AF-MWNT incorporated into the reaction and migrated to top aqueous layer was 55%. The value was reproducible.

PANi prepared from oxidative polymerization in water (see Supporting Information Fig. S3).

Transmission Electron Microscopy (TEM)

Both samples were dispersed in NMP and then the carbon coated grid was dipped into the mixture and taken out to dry in a vacuum oven. The morphology of PANi is indeed nanofiber, which has diameter of ~50 nanometers without concentric hollow interior [Fig. 5(a)]. Compared to SEM images [see Fig. 4(a,b)], the increment of diameter dimension should be due to the flattened morphology of PANi nanofiber after swollen in NMP. Fuzzy image of the flat area further confirmed the diameter increase in the flattened PANi nanofibers [Fig. 5(b)]. The TEM images of PANi/PANi-*g*-MWNT show that the MWNTs are heavily decorated with PANi [Fig. 5(c,d)]. Furthermore, the distinct wall-to-wall stripes of MWNTs framework and grafting of PANi were clearly observed at high magnification [Fig. 5(d), inset]. The covalent attachment of the PANi onto the AF-MWNT could be visually verified. The basic structure of MWNT remained intact during all reaction and work-up handling could also be assured. Hence, it could be concluded that some PANi was efficiently grafted onto the surface of the AF-MWNT to afford PANi/PANi-*g*-MWNT mixture. The microscopic study affirmed that

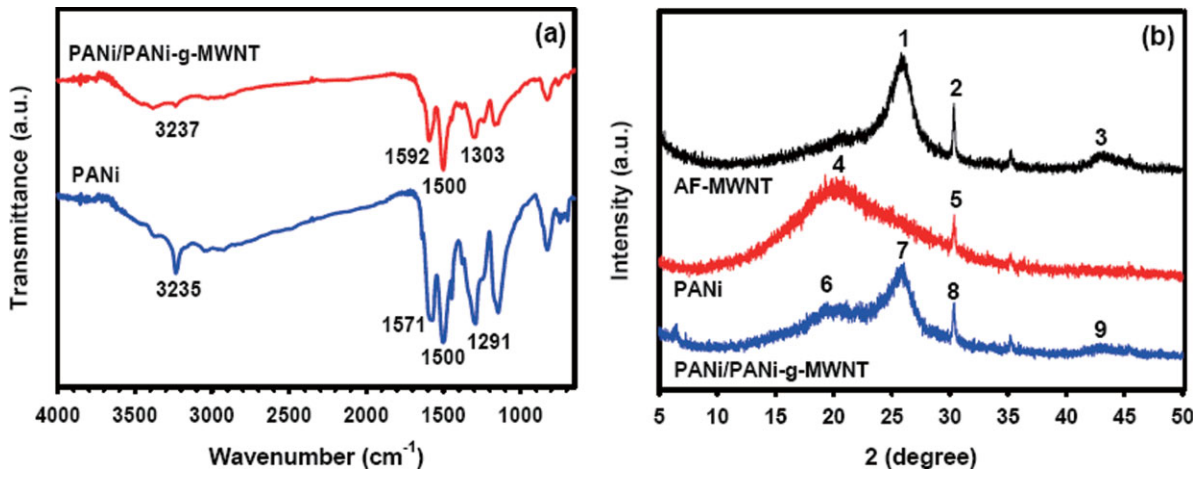

FIGURE 3 (a) FTIR (KBr pellet) spectra of PANi and PANi/PANi-*g*-MWNT; (b) X-ray diffraction patterns of AF-MWNT, PANi and PANi/PANi-*g*-MWNT.

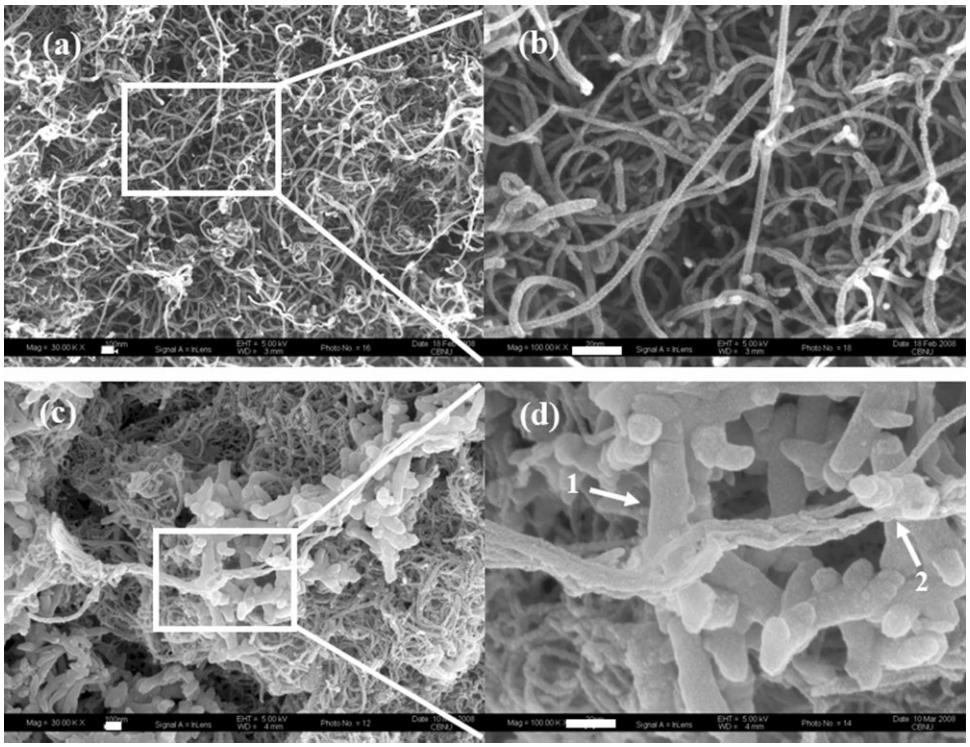

FIGURE 4 SEM images of samples: (a) PANi (30,000×); (b) PANi (100,000×); (c) PANi/PANi-*g*-MWNT (30,000×); (d) PANi/PANi-*g*-MWNT (100,000×). Scale bars are 100 nm.

MWNT could sustain intact structure during functionalization in a mildly acidic PPA medium or graft-polymerization in an aqueous acidic medium. In addition to both reaction sequences, MWNT framework maintained its structural integrity throughout work-up procedures at each reaction step. The unique results from SEM and TEM explained that the reaction conditions applied in this work are indeed effective to functionalize MWNTs and synthesize PANi/PANi-*g*-MWNT mixture.

BET Surface Area

To measure surface area using the BET method, the PANi and PANi/PANi-*g*-MWNT mixture were dedoped into 1 M aqueous ammonium hydroxide to minimize the effect of the dopants and then the powder samples were degassed under vacuum at 100 °C before measurement. The surface areas of PANi and PANi/PANi-*g*-MWNT were 52.56 and 85.20 m^2/g, respectively (see Supporting Information Table 2 and Fig. S4). The surface area of PANi/PANi-*g*-MWNT was increased

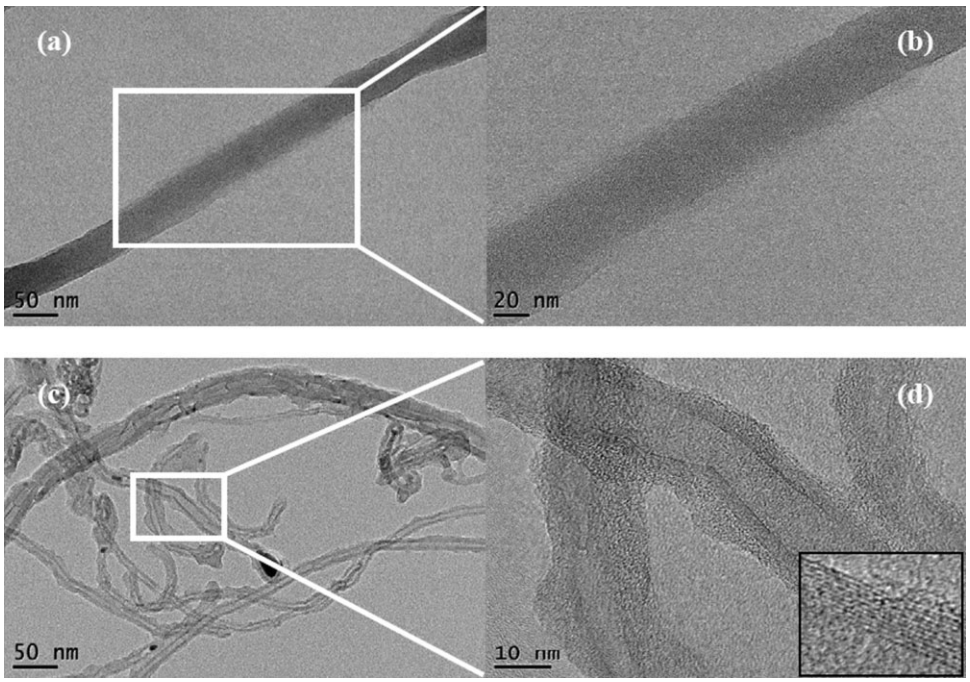

FIGURE 5 TEM images of samples: (a) PANi (50,000×); (b) PANi (100,000×); (c) PANi/PANi-*g*-MWNT (50,000×); (d) PANi/PANi-*g*-MWNT (300,000×).

TABLE 2 BET Surface Area, Pore Volume and Average Pore Size of PANi and PANi-*g*-MWNT

Sample	Surface Area (m^2/g)	Pore Volume (mL/g)	Pore Size (Å)
Dedoped PANi	52.56	0.01152	150.52
Dedoped PANi/ PANi-*g*-MWNT	85.20	0.00358	208.35

by ~62%. Together with WAXD and SEM results [see Figs. 3(b) and 4(f)], this result further supported that AF-MWNT had provided grafting and nucleating sites to PANi. As a result, the average diameter of PANi-*g*-MWNT became very large (approximately 80–90 nm), while relatively shorter PANi nanofibers were formed in the presence of AF-MWNT compared with PANi nanofibers [see Fig. 4(c,d)].

Thermo-Oxidative Stability

When TGA was run in dry air atmosphere. dedoped PANi and PANi/PANi-*g*-MWNT underwent 5% weight loss ($T_{d5\%}$) at 343 and 386 °C, respectively (Fig. 6), indicating that the thermo-oxidative stability of PANi/PANi-*g*-MWNT was ~43 °C higher than that of PANi homopolymer. However, the char yields at 800 °C were almost 0% for both samples.

UV-Vis Absorption and Emission Studies

UV-Vis absorption and emission measurements were used to characterize the interfacial interaction between PANi and MWNT. Stock solutions (10.0 mg/L) were prepared by dissolving each sample in NMP. The UV-absorption of PANi showed two peaks at 336 and 623 nm [Fig. 7(a)]. The peaks are related to the $\pi \rightarrow \pi^*$ transition of benzenoid ring and quinoid ring, respectively, which are identical to that of dedoped PANi.[31] Based on this result, we believed that HCl dopants were mostly removed from PANi and PANi/PANi-*g*-MWNT samples in the process of Soxhlet extraction. In the case of PANi/PANi-*g*-MWNT mixture, a single peak at 326 nm was detected and it was blue-shifted by 10 nm compared to that of PANi homopolymers. Interestingly, the peak related to the $\pi \rightarrow \pi^*$ transition of quinoid ring did not appear in the PANi/PANi-*g*-MWNT solution. This result implied that the peak had disappeared because of the intimate interaction between quinoid ring and MWNT. The interaction should be closely related to the observed conductivity of PANi/PANi-*g*-MWNT mixture, since MWNT could serve as nonvolatile electron deficient dopant as well as conducting bridge.

For fluorescent measurements, samples were excited at the UV absorption wavelength maxima. The emission maxima of PANi and PANi/PANi-*g*-MWNT were at 410 and 403 nm, respectively [Fig. 7(b)]. The peak wavelength of PANi/PANi-*g*-MWNT was slightly blue-shifted and the peak intensities of both samples were similar. This suggest that most of MWNT should be covalently decorated by PANi. If AF-MWNT and PANi were physically aggregated by intermolecular π-π interaction in solid state and segregated in solution, the emission intensity of PANi/PANi-*g*-MWNT should be much weaker and the peak location should be quite shifted because MWNT could act as strong excimer quencher and light absorber as well.[32]

Cyclic Voltammetry

Cyclic voltammetry (CV) is generally used to investigate the electrochemical properties of conductive materials. Thus, PANi and PANi/PANi-*g*-MWNT were characterized by CV using a three-electrode electrochemical cell. PANi and PANi/PANi-*g*-MWNT show oxidation and reduction peaks at ~0.5 and 0.3 V versus Ag/AgCl, respectively [Fig. 8(a)]. These values corresponded to the processes, in which PANi undergoes two sequential single-electron transfer processes.[33] Also, they displayed well-defined redox process from the first to tenth scan. It could be observed that the output current of PANi/PANi-*g*-MWNT mixture was significantly larger than that of PANi homopolymer. The capacitance can be estimated from the output current divided by the scan rate, indicating that the specific capacitance of PANi/PANi-*g*-MWNT was much larger than that of PANi homopolymer. In addition, the charge density loss of PANi/PANi-*g*-MWNT with respect to cycle number is less than that of PANi homopolmer [Fig. 8(b)]. The result supported that ion inclusion and exclusion in PANi/PANi-*g*-MWNT were more efficient during the redox process.

Resistivity Study

The resistivity was determined by the following equation $\sigma = 1/(\rho^*cf^*d)$, where σ, ρ, cf, and d are the conductivity, the resistivity, correction factor (4.340), and sample thickness in that order.[34] The calculated conductivity of as-prepared PANi/PANi-*g*-MWNT was 9.5 S/cm. The value was ~480 times higher than the value (1.97×10^{-2} S/cm) obtained from as-prepared PANi homopolymer (Table 3). The conductivity of PANi homopolymer after Soxhlet extraction (most HCl had been removed) was catastrophically dropped to 9.62×10^{-7} S/cm, while that of PANi/PANi-*g*-MWNT was still steady at 8.8 S/cm. The difference was as high as ~7 orders of magnitude. Subsequently, the samples were converted into the base form by treatment with 1 M aqueous

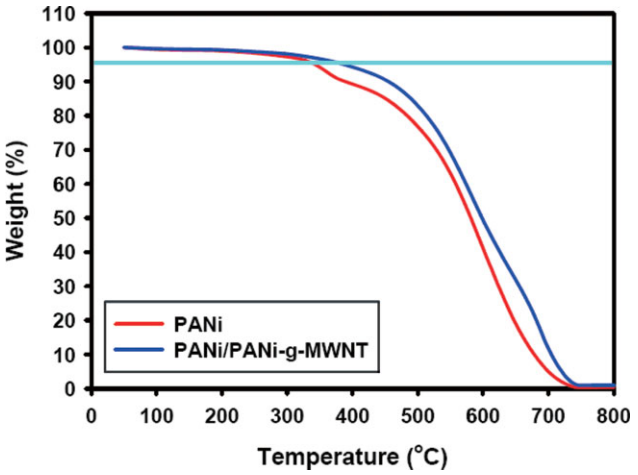

FIGURE 6 TGA thermograms of samples with heating rate of 10 °C/min in air. [Color figure can be viewed in the online issue, which is available at www.interscience.wiley.com.]

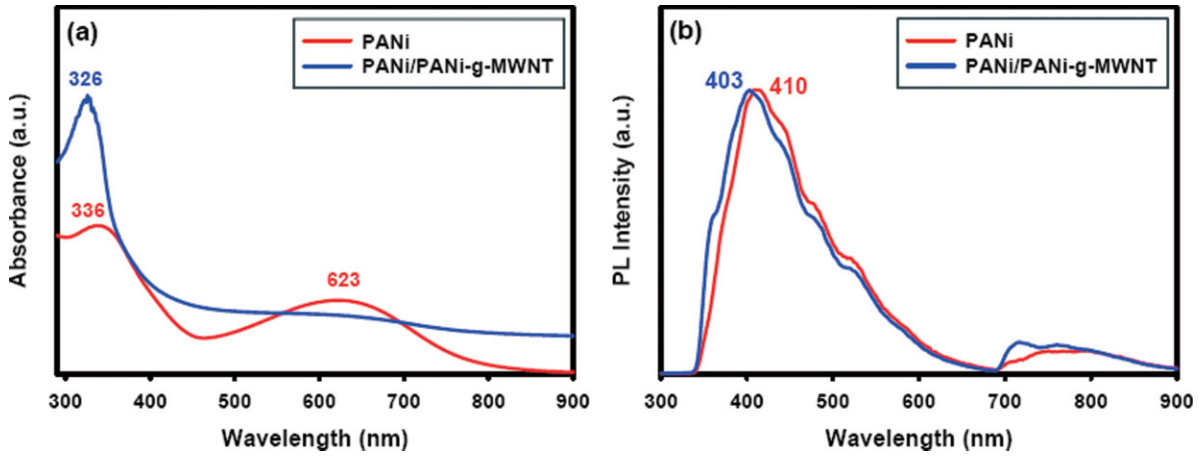

FIGURE 7 (a) UV-Vis absorption and (b) emission spectra of samples. [Color figure can be viewed in the online issue, which is available at www.interscience.wiley.com.]

ammonia to measure conductivities of dedoped PANi and PANi/PANi-*g*-MWNT. The measured conductivity of dedoped PANi was out of detection limit of the instrument (1×10^{-6} S/cm), whereas dedoped PANi/PANi-*g*-MWNT was still high in the semimetallic transport region at 4.9 S/cm. The resistivity of dedoped PANi is generally in the range of 10.0 M Ω cm–10.0 G Ω cm (1×10^{-7}–1×10^{-10} S/cm), which would classify PANi as an insulator without doping.[35] However, PANi/PANi-*g*-MWNT mixture displayed high conductivity regardless its doping states. The result implicated that MWNT played as outstanding nonvolatile dopant as well as conducting bridge.

In summary, the conductivity of resultant composites was significantly increased by hybridization of PANi and MWNT compared with PANi homopolymer. It could be explained that efficient charge transfer from the quinoid unit of PANi to the MWNT, which may serve as electron acceptors and conducting bridges.[17(c),36] Although reduced or neutral states of PANi displayed generally very low conductivity, the resultant mixture of PANi/PANi-*g*-MWNT displayed very good electrical conductivity regardless its doping states. While it has been demonstrated that CNT could play as a conductive dopant in CNT-based conducting polymer blend systems,[36,37] these systems involve inherent problems such as dispersion of CNT and interfacial interaction between CNT and polymer matrix. PANi/PANi-*g*-MWNT system does not appear to have these problems, because after PANi is covalently attached on the surface of MWNT, the PANi grafts would provide chemical affinity to effect the wrapping of free PANi to PANi-*g*-MWNT. In addition, mineral acid dopants such as hydrochloric, sulfuric, and nitric acids could migrate to the surface of PANi and then evaporate. Thus, the conductivity of doped PANi with passing time is generally decreased. On the other hand, MWNT could serve as permanent nonvolatile dopant in PANi/PANi-*g*-MWNT system.

CONCLUSIONS

MWNT was efficiently functionalized to afford a 4-aminobenzoyl-functionalized MWNT (AF-MWNT). PANi/PANi-*g*-MWNT mixture was synthesized via *in situ* static interfacial

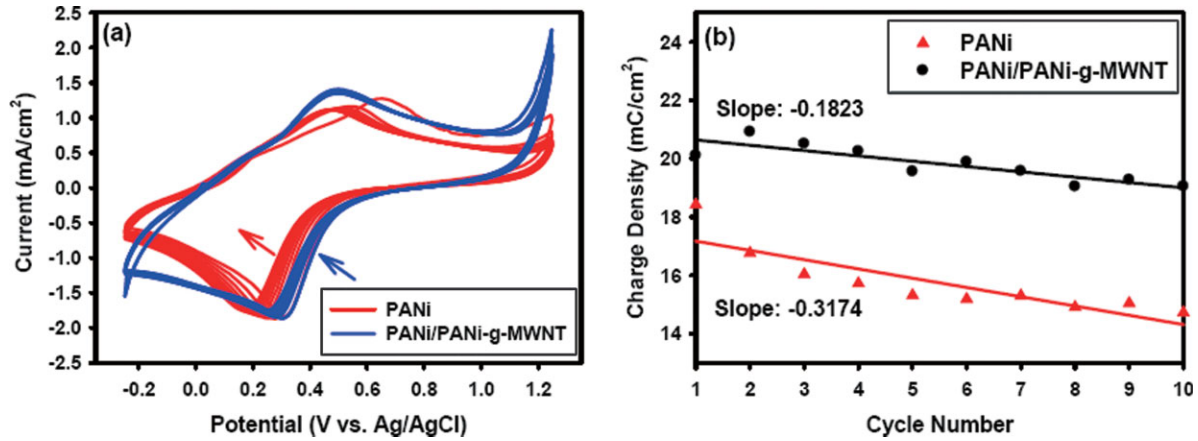

FIGURE 8 (a) Cyclic voltammograms of PANi and PANi/PANi-*g*-MWNT in 0.1 M H_2SO_4 aqueous solution. Scan rate is 10 mV/s; (b) charge density decay with respect to cycle time. [Color figure can be viewed in the online issue, which is available at www.interscience.wiley.com.]

TABLE 3 Conductivities of Samples with Respect to Doping States

State	Sample	Conductivity (S/cm)
Before Soxhlet extraction	PANi	1.97×10^{-2}
	PANi/PANi-*g*-MWNT	9.5
After Soxhlet extraction	PANi	9.62×10^{-7}
	PANi/PANi-*g*-MWNT	8.8
Dedoped with 1 M NH_4OH	PANi	Out of measuring limit
	PANi/PANi-*g*-MWNT	4.9

polymerization in the presence of AF-MWNT in organic phase. The structures and properties of PANi and PANi/PANi-*g*-MWNT were evaluated with a various analytical techniques such as FTIR, WAXD, SEM, TEM, TGA, UV-vis, and fluorescence. PANi/PANi-*g*-MWNT mixture displayed significantly improved conductivity and capacitance compared to PANi homopolymer. The results suggested that MWNT should play two important roles such as efficient electron acceptor and conducting bridge. After dedoping, the electrical conductivity of PANi was out of detection limit, but that of PANi/PANi-*g*-MWNT mixture still displayed very good electrical conductivity in "semimetallic" transport region at 4.9 S/cm. The PANI/PANI-*g*-MWNT mixture could be promising base material for many applications such as energy storage and sensors. Hence, the approach was indeed viable for the hybridization of various carbon nanomaterials and functional polymers to achieve synergistic enhancement stemmed from each component.

This project was supported by funding from World Class University (WCU) program supported by National Research Foundation (NRF) and Ministry of Education, Science and Technology (MEST) of Korea, US Air Force Office of Scientific Research, Asian Office of Aerospace R&D (AFOSR-AOARD).

REFERENCES AND NOTES

1 (a) Skotheim, T. A.; Elsenbaumer, R. L.; Reynolds, J. R. Handbook of Conducting Polymer, 2nd ed., Marcel Dekker, New York, 1997; (b) Bakhshi, A. K. Bull Mater Sci 1995, 18, 469–495.

2 (a) Huang, W. S.; Humphrey, B. D.; MacDiarmid, A. G. J Chem Soc Faraday Trans 1986, 82, 2385–2400; (b) Huang, J.; Moore, J. A.; Acquaye, J. H.; Kaner, R. B. Macromolecules 2005, 38, 317–321; (c) MacDiarmid, A. G. Angew Chem Int Ed 2001, 40, 2581–2590.

3 (a) Anderson, M. R.; Mattes, B. R.; Reiss H.; Kaner, R. B. Science 1991, 252, 1412–1415; (b) Cao, Y.; Smith P.; Heeger, A. J. Synth Met 1993, 57, 3514–3519; (c) Chiang J. C.; MacDiarmid, A. G. Synth Met 1986, 13, 193–205.

4 (a) DeBerry, D. W. J Electrochem Soc 1985, 132, 1022–1026; (b) Mengoli, G.; Musiani, M. M.; Pelli B.; Vecchi, E. J Appl Polym Sci 1983, 28, 1125–1136.

5 MacDiarmid, A. G.; Yang, L. S.; Huang, W. S.; Humphrey, B. D. Synth Met 1987, 18, 393–398.

6 (a) Yan, X. B.; Han, Z. J.; Yang Y.; Tay, B. K. Sens Actuators B 2007, 123, 107–113; (b) Janata J. Josowicz, M. Nat Mater 2003, 2, 19–24.

7 (a) Trivedi D. C.; Dhawan, S. K. J Mater Chem 1992, 2, 1091–1096; (b) Maziarz, E. P.; Lorenz, S. A.; White, T. P.; Wood, T. D. J Am Soc Mass Spectro 2000, 11, 659–663.

8 (a) Wang, Y.; Liu, Z.; Han, B.; Sun, Z.; Huang Y.; Yang, G. Langmuir 2005, 21, 833–836; (b) Ding, H.; Wan M.; Wei, Y. Adv Mater 2007, 19, 465–469.

9 Niu, Z.; Yang, Z.; Hu, Z.; Lu, Y.; Han, C. C. Adv Funct Mater 2003, 13, 949–954.

10 Qiu, H.; Wan, M.; Matthew, B.; Dai, L. Macromolecules 2001, 34, 675–680.

11 Wei, Z.; Wan, M. Adv Mater 2002, 14, 1314–1317.

12 (a) Chiou N. R.; Epstein, A. Adv Mater 2005, 17, 1679–1979; (b) Chiou N. R.; Epstein, A. Synth Met 2005, 153, 69–72.

13 (a) Huang, J.; Virji, S.; Weiller, B. H.; Kaner, R. B. J Am Chem Soc 2003, 125, 314–315; (b) Huang J.; Kaner, R. B. J Am Chem Soc 2004, 126, 851–855; (c) Huang J. X.; Kaner, R. B. Angew Chem Int Ed 2004, 43, 5817–5821.

14 (a) Gao, H.; Jiagn, T.; Han, B.; Wang, Y.; Du. J.; Liu, Z.; Zhang, J. Polymer 2004, 45, 3017–3019; (b) Zhang, X.; Chan-Yu-King, R.; Jose, A.; Manohar, S. K. Synth Met 2004, 145, 23–29.

15 (a) Frackowiak, E.; Khomenko, V.; Jurewica, K.; Lota, K.; Béguin, F. J Power Sources 2006, 153, 413–418; (b) Wu, M.; Snook, G. A.; Gupta, V.; Shaffer, M.; Fray, D. J.; Chen, G. Z. J Mater Chem 2005, 15, 2297–2303.

16 (a) Ajayan, P. M. Chem Rev 1999, 99, 1787–1800; (b) Sinnott, S. B. J Nanosci Nanotech 2002, 2, 113–123; (c) Zhao, Q.; Gan, Z.; Zhuang, Q. Electroanalysis 2002, 14, 1609–1613; (d) Ajayan P. M.; Zhou, Q. Z. Top Appl Phys 2001, 80, 391–425; (e) Baughman, R. H.; Zakhidov, A. A.; de Heer, W. A. Science 2002, 297, 787–792.

17 (a) Mottaghitalab, V.; Spinks, G. M.; Wallace, G. G. Synth Met 2005, 152, 77–80; (b) Qiao, Y.; Li, C. M.; Bao, S.-J.; Bao, Q.-L. J Power Sources 2007, 170, 79–84; (c) Zengin, H.; Zhou, W.; Jin, J.; Czerw, R.; Smith, D. W., Jr.; Echegoyen, L.; Carroll, D. L.; Foulger, S. H.; Ballato, J. Adv Mater 2002, 14, 1480–1483; (d) Zhao, H.; Yuan, W. Z.; Mei, J.; Tang, L.; Liu, X. Q.; Yan, J. M.; Shen, X. Y.; Sun, J. Z.; Qin, A.; Tang, B. Z. J Polym Sci Part A: Polym Chem 2009, 47, 4995–5005.

18 (a) Chen, J.; Rao, A. M.; Lyuksyutov, S.; Itkis, M. E.; Hamon, M. A.; Hu, H.; Cohn, R. W.; Eklund, P. C.; Colbert, D. T.; Smalley, R. E.; Haddon, R. C. J Phys Chem B 2001, 105, 2525–2528; (b) Ramesh, A.; Ericson, L. M.; Davis, V. A.; Saini, R. K.; Kittrell, C.; Pasquali, M.; Billups, W. E.; Adams, W. W.; Hauge, R. H.; Smalley, R. E. J Phys Chem B 2004, 108, 8794–8798.

19 (a) Brodie, B. C. Ann Chim Phys 1860, 59, 466–472; (b) Hummers, W.; Offeman, R. J Am Chem Soc 1958, 80, 1339.

20 Price, B. K.; Lomeda, J. R.; Tour, J. M. Chem Mater 2009, 21, 3917–3923.

21 (a) Baek, J.-B.; Lyon, C. B.; Tan, L.-S. J Mater Chem 2004, 14, 2052–2056; (b) Han, S.-W.; Oh, S.-J.; Tan L.-S.; Baek, J.-B. Carbon 2008, 46, 1841–1849; (c) Lee, H.-J.; Han, S.-W.; Kwon, Y.-D.; Tan, L.-S.; Baek, J.-B. Carbon 2008, 46, 1850–1859; (d) Jeon, I.-Y.; Lee, H.-J.; Choi, Y. S.; Tan L.-S.; Baek, J.-B. Macromolecules 2008, 41, 7423–7432.

22 Sammalkorpi, M.; Krasheninnikov, A.; Kuronen, A.; Nordlund, K.; Kaski, K. Phys Rev B 2004, 70, 245416-1–245416-7.

23 http://hnt.hanwhananotech.co.kr.

24 Baek, J.-B.; Tan, L.-S. Polymer 2003, 44, 4135–4147.

25 Lee, H.-J.; Oh, S.-J.; Choi, J.-Y.; Kim, J.-W.; Han, J.; Tan, L.-S.; Baek, J.-B. Chem Mater 2005, 17, 5057–5064.

26 (a) Ebbesen, T. W.; Takada, T. Carbon 1995, 33, 973–978; (b) Meunier, V.; Lambin, P. Carbon 2000, 38, 1729–1733; (c) Qian, W.; Liu, T.; Wei, F.; Wang, Z.; Luo, G.; Yu, H.; Li, Z. Carbon 2003, 41, 2613–2617; (d) Shimada, T.; Yanase, H.; Morishita, K.; Hayashi, J.; Chiba, T. Carbon 2004, 42, 1635–1639.

27 Chen, J.; Shan, J. Y.; Tsukada, T.; Munekane, F.; Kuno, A.; Matsuo, M.; Hayashi, T.; Kim, Y. A.; Endo, M. Carbon 2007, 45, 274–280.

28 Łużny, W.; Śniechowski, M.; Laska, J. Synth Met 2002, 126, 27–35.

29 Chen, S. A.; Lee, H. T. Macromolecules 1993, 26, 3254–3261.

30 Jiaxing, H.; Richard, B. K. J Am Chem Soc 2004, 126, 851–855.

31 (a) Wan, M. X. Synth Met 1989, 31, 51–59; (b) Guicun, L.; Li, J.; Hongrui, P. Macromolecules 2007, 40, 7890–7894; (c) Wang, Y. Jing, X. Polym Test 2005, 24, 153–156.

32 Feng, W.; Fujii, A.; Ozaki, M.; Yoshino, K. Carbon 2005, 43, 2501–2507.

33 (a) Chen, R.; Benicewicz, B. C. Macromolecules 2003, 36, 6333–6339; (b) Sadighi, J. P.; Singer, R. A.; Buchwald, S. L. J Am Chem Soc 1998, 120, 4960–4976.

34 Perloff, D. S. Solid State Electron 1977, 20, 681–687.

35 (a) Bianchi, R. F.; Leal Ferreira, G. F.; Lepienski, C. M.; Faria, R. M. J Chem Phys 1999, 110, 4602–4707; (b) Chaudhari, H. K.; Kelkar, D. S. Polym Int 1997, 42, 380–384; (c) Zilberman, M.; Titelman, G. I.; Siegmann, A.; Haba, Y.; Narkis, M.; Alperstein, D. J Appl Polym Sci 1998, 66, 243–253.

36 Wu, T.-M.; Lin, Y.-W.; Liao, C.-S. Carbon 43, 734–740.

37 (a) Chen, G. Z.; Shaffer, M. S.; Coleby, D.; Dixon, G.; Zhou, W.; Fray, D. J.; Windle, A. H. Adv Mater 2000, 12, 522–526; (b) Luo, X.; Killard, A. J.; Morrin, A.; Smyth, M. R. Anal Chim Acta 2006, 575, 39–44.